nature medicine

Clearance of senescent cells by ABT263 rejuvenates aged hematopoietic stem cells in mice

Jianhui Chang[1,2,9], Yingying Wang[1–3,9], Lijian Shao[1,2], Remi-Martin Laberge[4], Marco Demaria[4], Judith Campisi[4,5], Krishnamurthy Janakiraman[6], Norman E Sharpless[6], Sheng Ding[7], Wei Feng[1,2], Yi Luo[1,2], Xiaoyan Wang[1,2], Nukhet Aykin-Burns[1,2], Kimberly Krager[1,2], Usha Ponnappan[8], Martin Hauer-Jensen[1,2], Aimin Meng[3] & Daohong Zhou[1,2]

Senescent cells (SCs) accumulate with age and after genotoxic stress, such as total-body irradiation (TBI)[1–6]. Clearance of SCs in a progeroid mouse model using a transgenic approach delays several age-associated disorders[7], suggesting that SCs play a causative role in certain age-related pathologies. Thus, a 'senolytic' pharmacological agent that can selectively kill SCs holds promise for rejuvenating tissue stem cells and extending health span. To test this idea, we screened a collection of compounds and identified ABT263 (a specific inhibitor of the anti-apoptotic proteins BCL-2 and BCL-xL) as a potent senolytic drug. We show that ABT263 selectively kills SCs in culture in a cell type– and species-independent manner by inducing apoptosis. Oral administration of ABT263 to either sublethally irradiated or normally aged mice effectively depleted SCs, including senescent bone marrow hematopoietic stem cells (HSCs) and senescent muscle stem cells (MuSCs). Notably, this depletion mitigated TBI-induced premature aging of the hematopoietic system and rejuvenated the aged HSCs and MuSCs in normally aged mice. Our results demonstrate that selective clearance of SCs by a pharmacological agent is beneficial in part through its rejuvenation of aged tissue stem cells. Thus, senolytic drugs may represent a new class of radiation mitigators and anti-aging agents.

Previous efforts to identify small molecules that selectively kill SCs have yielded only two nonspecific and cell type–selective senolytic drugs[8]. To identify senolytic drugs that are more specific and have broader-spectrum activity, we took a targeted approach by individually titrating the cytotoxicity of a handful of small molecules that participate in pathways predicted to be important for the viability of SCs or for the maintenance of their phenotype (**Supplementary Tables 1** and **2**). We studied the effects of these compounds on human WI-38 fibroblasts, because this cell line has been extensively used to study replicative and stress-induced premature senescence in culture[9,10]. After incubation with the compounds, we assessed the survival of WI-38 cells that either were non-senescent or that had been induced to senesce by treatment with ionizing radiation (IR), replicative exhaustion or oncogenic *Ras* expression. Using this approach, we identified ABT263 as a potent senolytic drug that selectively, potently and rapidly kills SCs, regardless of how they were induced (**Fig. 1a**,**b** and **Supplementary Fig. 1**). In addition, ABT263 treatment was cytotoxic against SCs in a cell type– and species-independent manner: senescent human fibroblasts (IMR-90), human renal epithelial cells (RECs) and mouse embryo fibroblasts (MEFs) were more sensitive to ABT263 treatment than were their non-senescent counterparts (**Fig. 1c**).

To determine whether ABT263 is senolytic *in vivo*, we used sublethally irradiated p16-3MR transgenic mice. These mice carry a trimodal reporter protein (3MR) under the control of the cyclin-dependent kinase inhibitor 2a (*Cdkn2a*; also referred to as *p16*) promoter (**Supplementary Fig. 2a**)[11]. p16 is a widely used SC biomarker and a modulator of stem cell aging[12–14]. The 3MR-encoding transgene encodes a fusion protein consisting of *Renilla* luciferase (for bioluminescent imaging), monomeric red fluorescent protein (mRFP, for sorting and fluorescence microscopy) and herpes simplex virus thymidine kinase (HSV-TK, which converts ganciclovir (GCV) into a toxic DNA chain terminator to selectively kill HSV-TK–expressing SCs[11]). Therefore, p16-3MR mice can be used to identify, track and selectively kill $p16^+$ SCs *in vivo*. By whole-body luminescence imaging, exposure of young (2-month-old) p16-3MR mice to a sublethal dose (6 Gy) of TBI induced a time-dependent increase in SC abundance (**Supplementary Fig. 2b**,**c**). Non-irradiated p16-3MR mice showed little SC accumulation (as determined by luminescence) up to 8 months of age (data not shown). These findings agree with observations that SCs are rare in normal mice before 40 weeks of age, but rapidly accumulate after exposure to genotoxic insults[12,13]. After TBI, the lungs showed the greatest increase in SCs, and skeletal

[1]Department of Pharmaceutical Sciences, University of Arkansas for Medical Sciences, Little Rock, Arkansas, USA. [2]Winthrop P. Rockefeller Cancer Institute, University of Arkansas for Medical Sciences, Little Rock, Arkansas, USA. [3]Institute of Radiation Medicine, Peking Union Medical College (PUMC), Chinese Academy of Medical Sciences (CAMS), Tianjin, China. [4]Buck Institute for Research on Aging, Novato, California, USA. [5]Lawrence Berkeley National Laboratory, Berkeley, California, USA. [6]Department of Medicine and Genetics, University of North Carolina at Chapel Hill, Chapel Hill, North Carolina, USA. [7]Gladstone Institute of Cardiovascular Disease, San Francisco, California, USA. [8]Department of Microbiology and Immunology, University of Arkansas for Medical Sciences, Little Rock, Arkansas, USA. [9]These authors contributed equally to this work. Correspondence should be addressed to D.Z. (dzhou@uams.edu).

Received 27 August; accepted 16 November; published online 14 December 2015; doi:10.1038/nm.4010

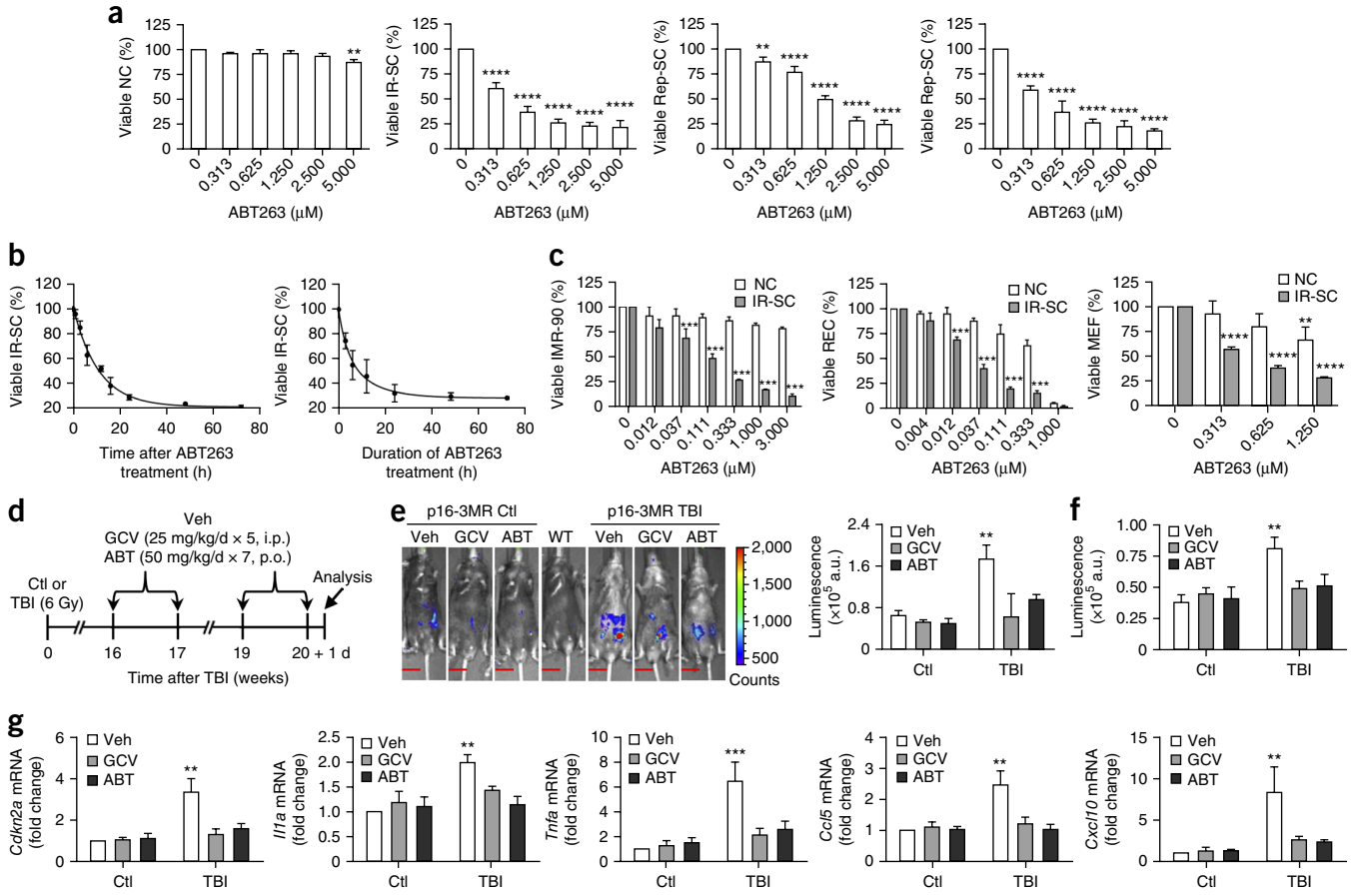

Figure 1 ABT263 has senolytic activity in cell culture and mice. (**a**) Quantification of viable WI-38 non-senescent cells (NC), IR-induced senescent cells (IR-SC), replication-exhausted senescent cells (Rep-SC) or Ras-induced senescent cells (Ras-SC; in which oncogenic Ras is ectopically expressed) 72 h after treatment with increasing concentrations of ABT263 ($n = 3$–6 for NC and IR-SC; $n = 3$ for Rep-SC; $n = 4$ for Ras-SC). (**b**) Quantification of viable IR-SCs at the indicated times after treatment of the IR-SCs with 1.25 μM ABT263 (left) or after the cells had been incubated with 1.25 μM ABT263 for the indicated amounts of time followed by removal of the drug and a further culture period of 72 h (right) ($n = 3$). (**c**) Quantification of viable non-senescent (NC) and IR-induced senescent (IR-SC) human IMR-90 fibroblasts (IMR-90), human renal epithelial cells (REC) and mouse embryonic fibroblasts (MEF) 72 h after treatment with increasing concentrations of ABT263 ($n = 3$ per group). (**d**) Experimental design for **e**–**g**. Sham-irradiated (Ctl) and TBI-treated young male p16-3MR mice were administered vehicle (Veh), ganciclovir (GCV) or ABT263 (ABT) and analyzed as indicated. I.p., intraperitoneal injection; p.o., oral administration. (**e**) Left, representative luminescence images of Ctl and TBI mice after treatment with vehicle, GCV or ABT263. Right, quantification (in arbitrary units, a.u.) of whole-body luminescence (Ctl mice: vehicle-treated, $n = 6$; GCV-treated, $n = 4$; ABT263-treated, $n = 6$; TBI mice: vehicle-treated, $n = 8$; GCV-treated, $n = 4$; ABT263-treated, $n = 7$). A wild-type C57BL/6 mouse (WT) was included as a negative control. The vertical color bar indicates luminescence-signal strength. Scale bars, 15 mm. (**f**) Quantification of luminescence in lungs of Ctl or TBI mice treated as indicated ($n = 5$ per group). (**g**) Quantification of mRNA expression for *Cdkn2a*, *Il1a*, *Tnfa*, *Ccl5* and *Cxcl10* in lungs from Ctl or TBI mice treated as indicated ($n = 4$ per group). Throughout, data are means ± s.e.m. $^{**}P < 0.01$, $^{***}P < 0.001$ and $^{****}P < 0.0001$ versus without ABT263 for **a** (one-way analysis of variance (ANOVA)); versus NC treated with the same concentrations of ABT263 for **c**; versus Ctl for **e**–**g**; two-way ANOVA for **c**–**g**.

muscle and brain showed the next greatest increase; liver and heart showed minimal increases (**Supplementary Fig. 2d**,**e**). Two GCV treatment cycles effectively cleared the SCs that had been induced by TBI of p16-3MR mice; notably, ABT263 treatment had a similar effect (**Fig. 1d**,**e**). SC clearance was confirmed by analyzing the lungs, in which GCV or ABT263 treatment not only reduced IR-induced SCs (**Fig. 1f**) but also suppressed the expression of several senescence-associated secretory phenotype (SASP) factors[15] (**Fig. 1g**). Thus, treatment with ABT263 was as effective as treatment with GCV in clearing IR-induced SCs in irradiated p16-3MR mice.

ABT263 is a potent inducer of apoptosis in many types of tumor cells[16]. To determine whether ABT263 induces apoptosis in SCs, we assayed apoptosis in IR-induced WI-38 SCs after vehicle or ABT263 treatment in the presence or absence of the pan-caspase inhibitor Q-VD-OPh (QVD)[17]. The selective killing of SCs by ABT263 treatment was abrogated in the presence of QVD (**Fig. 2a**,**b**), indicating that ABT263 killing depends on the induction of apoptosis. QVD treatment also protected IR-induced senescent IMR-90 fibroblasts and RECs against ABT263 cytotoxicity (**Supplementary Fig. 3a**,**b**). Irradiated WI-38 cells acquired sensitivity to ABT263 only after they became fully senescent, as determined by expression of senescence-associated β-galactosidase (SA–β-gal) (**Fig. 2c**). This result indicates that senescence, rather than DNA damage *per se*, sensitizes cells to ABT263. ABT263 probably kills SCs through the intrinsic apoptotic pathway[18,19], because treated SCs showed increased levels of activated caspase-3 but not of caspase-8 or receptor-interacting protein (RIP) 1 (**Fig. 2d**,**e**).

To determine whether SCs are more sensitive to ABT263 than non-senescent cells owing to differential expression of anti- or pro-apoptotic proteins, as suggested by previous studies[19,20], we

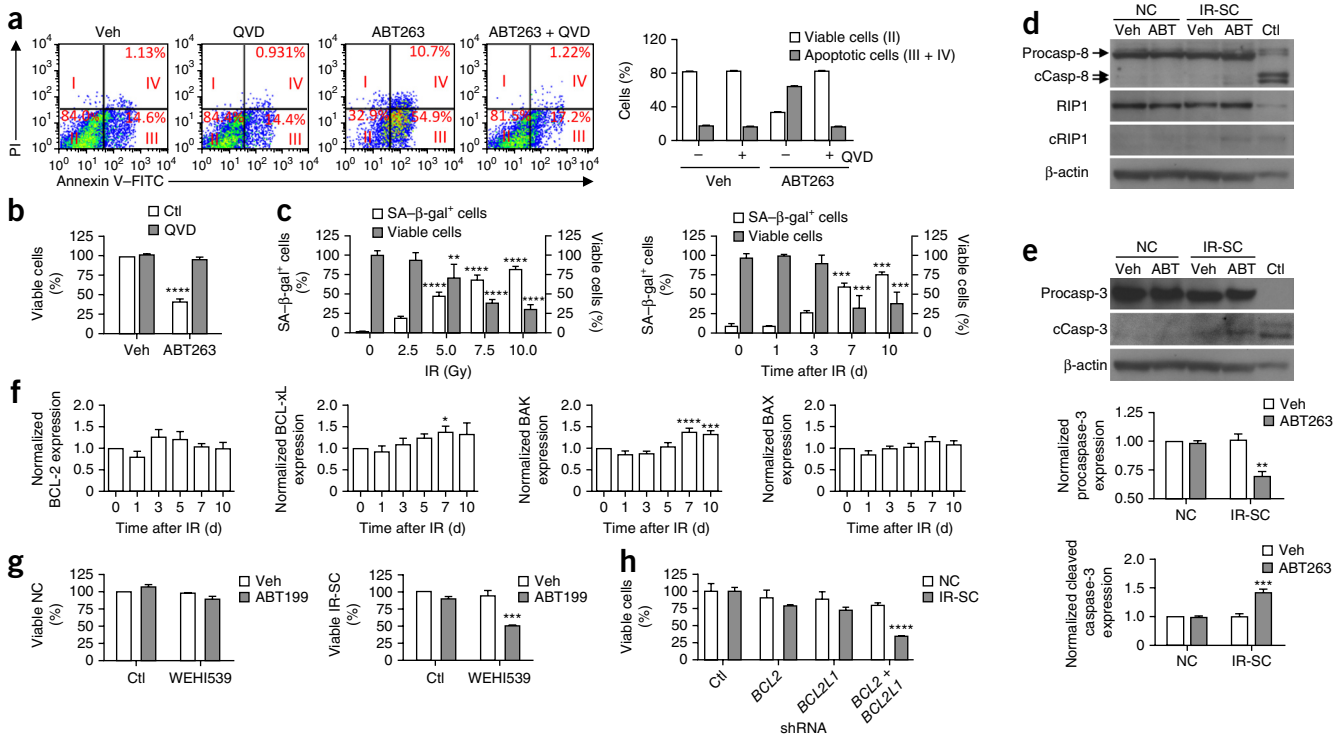

Figure 2 ABT263 kills SCs by apoptosis. (**a**) Representative flow cytometric plots to measure apoptosis (left) and quantitation of the percentage of viable (gate II: PI^-annexin V^-) and apoptotic (gates III and IV: PI^-annexin V^+ and PI^+annexin V^+) (right) cells of WI-38 IR-SC 24 h after treatment with vehicle (Veh), 1.25 μM ABT263, 20 μM Q-VD-Oph (QVD), or the combination of ABT263 and QVD. (**b**) Quantification of the percentage of viable IR-SC 72 h after treatment with vehicle or ABT263 ± QVD as in **a**. (**c**) Quantification of SA–β-gal^+ cells (white bars) 10 d after exposure to increasing doses of IR (left) or after increasing periods of time after treatment with 10 Gy IR (right), and the viability of the irradiated cells under these conditions after an additional incubation with 1.25 μM ABT263 for 72 h (gray bars). (**d**) Representative western blot analysis of procaspase-8 (Procasp-8), cleaved caspase-8 (cCasp-8), RIP1, cleaved RIP1 (cRIP1) and β-actin in NC and IR-SC 24 h after incubation with vehicle or 1.25 μM ABT263 (ABT). (**e**) Top, representative western blot analysis of procaspase-3 (Procasp-3), cleaved caspase-3 (cCasp-3) and β-actin in NC and IR-SC from **d**. Bottom, normalized expression of Procasp-3 and cCasp-3 in NC and IR-SC. Because the samples used for the western blots in **d**,**e** were the same, the same β-actin blot was used as a control for both panels. A mixture of cell lysates from etoposide- or cytochrome c–treated Jurkat cells was used as a positive control (Ctl) for detection of cCasp-3 and cCasp-8. (**f**) Normalized expression of BCL-2, BCL-xL, BAK and BAX in WI-38 cells by western blot analysis at increasing times after treatment with IR (10 Gy). (**g**) Quantification of NC (left) and IR-SC (right) viability 72 h after incubation with vehicle, 2.5 μM ABT199, 0.625 μM WEHI539, or the combination of ABT199 and WEHI539. (**h**) Quantification of NC and IR-SC viability 72 h after transfection with a control shRNA (Ctl) or shRNAs specific for *BCL2*, *BCL2L1*, or both *BCL2* and *BCL2L1*. Throughout, data are means ± s.e.m. of three experiments, except for **h** ($n = 5$). $^*P < 0.05$, $^{**}P < 0.01$, $^{***}P < 0.001$ and $^{****}P < 0.0001$; one-way ANOVA for **c**,**f**; two-way ANOVA for **b**,**e**,**g**,**h**.

measured the levels of these proteins in SCs. ABT263 sensitivity correlated with increased expression of anti-apoptotic BCL-xL and pro-apoptotic BAK, but not with increased expression of anti-apoptotic BCL-2 or the pro-apoptotic BAX, BAD, BID, BIM or NOXA proteins (**Fig. 2f** and **Supplementary Fig. 3c**,**d**). Inhibition of BCL-2 or BCL-xL function alone by treating cells with ABT199 (ref. 21) or WEHI539 (ref. 22), respectively, did not selectively kill SCs; however, treatment with the combination of ABT199 and WEHI539 did so (**Fig. 2g** and **Supplementary Fig. 3e**,**f**). This finding suggests that BCL-2 and BCL-xL act in a redundant manner to protect SCs from apoptotic death, such that simultaneous inhibition of BCL-2 and BCL-xL activity is required to selectively induce SC apoptosis. Consistent with this idea, downregulation of *BCL2* or *BCL2L1* (which encode BCL-2 and BCL-xL, respectively) expression by using short hairpin RNAs (shRNAs) specific for these transcripts had minimal effects on SC survival, but downregulation of both *BCL2* and *BCL2L1* expression selectively reduced SC viability (**Fig. 2h**).

Our previous studies[4] showed that sublethal TBI induces long-term bone marrow injury that is manifested by a persistent decrease in HSC self-renewal and hematopoietic function. This effect is probably mediated by induction of HSC senescence, as HSCs from TBI-treated mice exhibited increases in mRNA expression of *Cdkn1a* (another commonly used biomarker for SCs) and *Cdkn2a*, an increase in SA–β-gal staining and a decrease in clonogenic activity (**Supplementary Fig. 4**). Senescent HSCs induced by IR treatment exhibited phenotypes similar to those seen in HSCs from aged animals, including decreases in self-renewal, clonogenicity and long-term repopulating ability, as well as myeloid skewing[4,23–26]. Therefore, IR-induced long-term bone marrow injury can be considered to represent a model of premature aging of the hematopoietic system[4,23–29]. In addition, long-term bone marrow injury in irradiated patients can promote, over time or after additional hematopoietic stress, hypoplastic anemia, myelodysplastic syndrome or leukemia[30–32].

Using our sublethal TBI C57BL/6 mouse model[4], we asked whether ABT263 treatment can effectively clear SCs, including senescent HSCs induced by IR treatment, and whether SC clearance can rejuvenate the prematurely aged hematopoietic system and/or mitigate IR-induced long-term bone marrow injury. Bone marrow HSCs from irradiated

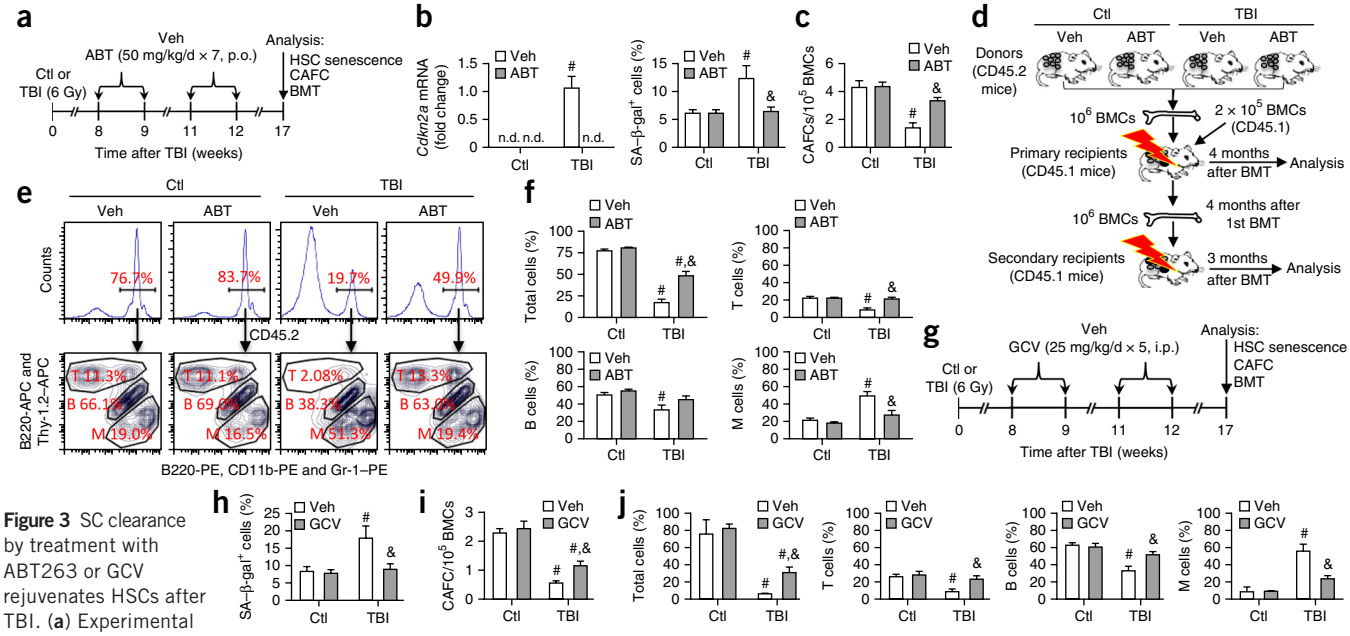

Figure 3 SC clearance by treatment with ABT263 or GCV rejuvenates HSCs after TBI. (**a**) Experimental design for **b**–**f**. Sham-irradiated (Ctl) and TBI-treated young male C57BL/6 mice were administered vehicle (Veh) or ABT263 (ABT) and analyzed as indicated. (**b**,**c**) Quantification of changes in *Cdkn2a* mRNA levels (**b**, left; $n = 3$ biological replicates) and the percentage of SA–β-gal$^+$ cells (**b**, right; $n = 4$ mice per group) in sorted HSCs, and the number of day 35 cobblestone area–forming cells (CAFCs) in bone marrow cells (BMCs; **c**; $n = 4$ mice per group). $^{\#}P < 0.05$ versus Ctl mice; $^{\&}P < 0.05$ versus vehicle-treated TBI mice; two-way ANOVA; n.d., not detectable. (**d**) Scheme for competitive and serial bone marrow transplantation (BMT; see Online Methods for details). (**e**,**f**) Representative flow cytometry plots (**e**) and quantification (**f**) of donor-derived total white blood cells (CD45.2$^+$; **e**, top; **f**, top left), and T cells (T; CD45.2$^+$Thy-1.2$^+$), B cells (B; CD45.2$^+$B220$^+$) and myeloid cells (M cells; CD45.2$^+$CD11b/Gr-1$^+$) (**e**, bottom; **f**) in the peripheral blood (PB) of recipient mice after primary BMT ($n = 6$ recipients per group). Donor-cell engraftment in the PB of secondary recipients is shown in **Supplementary Figure 6**. (**g**) Experimental design for **h**–**j**. Sham-irradiated (Ctl) and TBI-exposed young male p16–3MR mice were treated with vehicle or GCV and analyzed as indicated. (**h**) Quantification of the percentages of SA–β-gal$^+$ cells in sorted HSCs from mice treated as outlined in **g** (Ctl mice: vehicle-treated, $n = 7$; GCV-treated, $n = 7$; TBI mice: vehicle-treated, $n = 11$; GCV-treated, $n = 12$). (**i**) Quantification of the number of day 35 CAFCs in BMCs (Ctl mice: vehicle-treated, $n = 3$; GCV-treated, $n = 3$; TBI mice: vehicle-treated, $n = 7$; GCV-treated, $n = 6$). (**j**) Quantification of the percentages of donor-derived total cells, T cells, B cells and M cells in the PB of primary recipients (Ctl donors: vehicle-treated, $n = 3$ recipients; GCV-treated, $n = 5$ recipients; TBI donors: vehicle-treated, $n = 7$ recipients; GCV-treated, $n = 9$ recipients). Throughout, data are means ± s.e.m. In **f**,**j**, $^{\#}P < 0.05$ versus recipients of donor-derived cells from Ctl mice; $^{\&}P < 0.05$ versus recipients of donor-derived cells from vehicle-treated TBI mice; in **h**,**i**, $^{\#}P < 0.05$ versus Ctl mice; $^{\&}P < 0.05$ versus vehicle-treated TBI mice; two-way ANOVA; n.d., not detectable.

control (vehicle-treated) mice showed significant increases in *Cdkn2a* mRNA and SA–β-gal levels, as compared to HSCs from sham-irradiated (Ctl) mice (**Fig. 3a**,**b**), indicating that sublethal TBI induces HSC senescence. As assessed by these markers, senescent HSCs were effectively cleared by ABT263 treatment. The clearance of senescent HSCs by treatment with ABT263 did not quantitatively reduce the percentages and numbers of HSCs and hematopoietic progenitor cells (HPCs) in the bone marrow (**Supplementary Fig. 5**). Instead, ABT263 treatment significantly improved the clonogenicity (**Fig. 3c**) and long-term engraftment ability of irradiated HSCs after transplantation into both primary and secondary recipients (**Fig. 3d**–**f** and **Supplementary Fig. 6**). In addition, ABT263 treatment (i) attenuated TBI-induced HSC myeloid skewing (**Fig. 3e**,**f** and **Supplementary Fig. 6**), a prominent aging phenotype; (ii) attenuated the disruption of HSC quiescence (as assessed by the percentage of HSCs in the G0 stage of the cell cycle), which can lead to premature exhaustion in HSCs; and (iii) reduced the numbers of HSCs with persistent DNA damage (**Supplementary Fig. 7**). The attenuation of myeloid skewing may be partly due to increased lymphopoiesis (**Supplementary Fig. 8**).

The mechanism by which ABT263 rejuvenates the prematurely aged hematopoietic system of irradiated mice appears to be primarily through the selective cytotoxicity of ABT263 against senescent HSCs, because ABT263 treatment had selective cytotoxic effects in culture against HSCs isolated from mice treated with TBI but had no effect on HSCs from non-irradiated control mice (**Supplementary Fig. 9a**). We suggest that clearance of senescent HSCs by ABT263 treatment can promote the expansion of normal HSC clones that were either spared from or had repaired IR-induced damage and were thus able to expand into the vacated HSC niche. ABT263 treatment also abrogated the IR-induced SASP response in HSCs and bone stromal cells (**Supplementary Fig. 9b**,**c**)[15,33]; this effect on the SASP response may also contribute to the rejuvenation of HSCs after TBI by improving the bone marrow microenvironment. To more critically test the idea that rejuvenation of the hematopoietic system of irradiated mice by ABT263 treatment is mediated by SC clearance, we used GCV treatment to specifically deplete SCs in p16-3MR mice after they had been exposed to 6 Gy TBI, in a manner similarly to that of ABT263 administration to C57BL/6 mice that had been treated with TBI (**Fig. 3a**,**g**). Depletion of SCs in irradiated p16-3MR mice by using GCV (**Fig. 3g**–**j**) phenocopied the findings for ABT263-treated TBI-exposed C57BL/6 mice (**Fig. 3b**–**f**,**h**–**j**), supporting the idea that the beneficial effects of ABT263 on the prematurely aged hematopoietic system induced by TBI treatment are mainly because of the killing of SCs.

Similarly to its effects in TBI-treated mice, ABT263 treatment cleared SCs in normally aged mice (**Fig. 4a**). Treatment with ABT263 also significantly reduced age-related increases in the mRNA levels

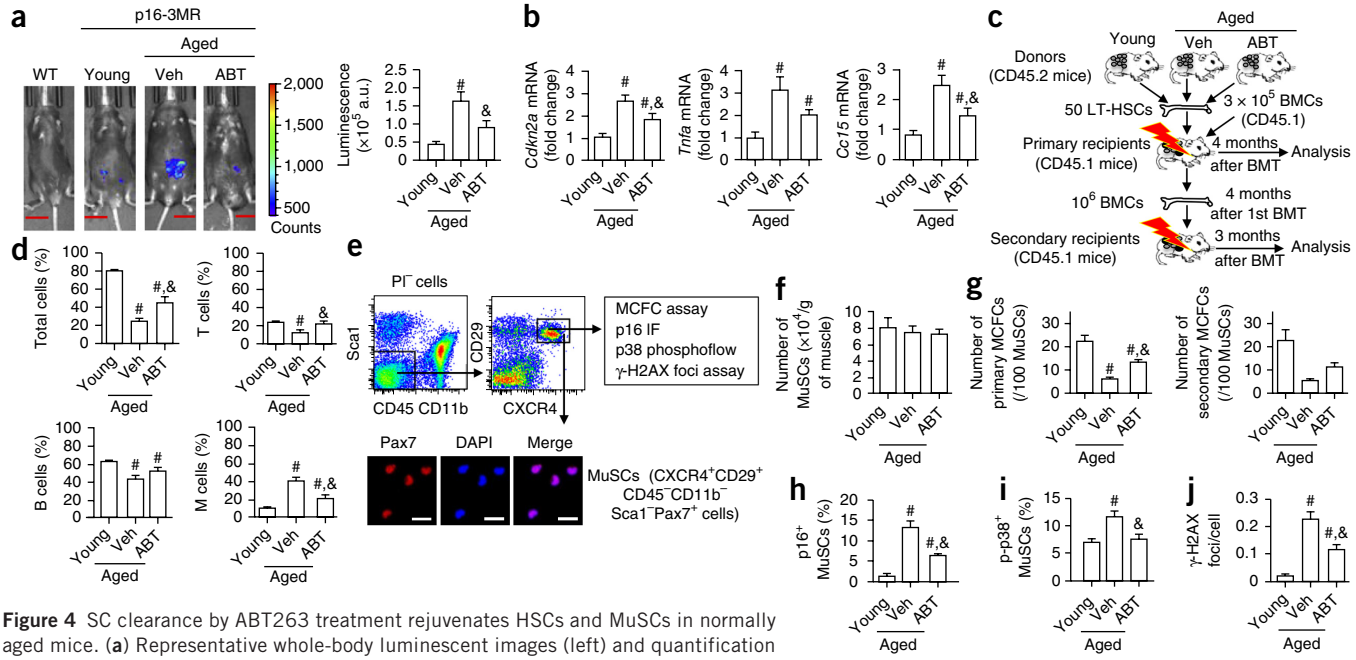

Figure 4 SC clearance by ABT263 treatment rejuvenates HSCs and MuSCs in normally aged mice. (**a**) Representative whole-body luminescent images (left) and quantification of luminescence (right) 1 d after 21- to 22-month-old male p16-3MR mice (aged) received vehicle (Veh; $n = 7$) or ABT263 (ABT; $n = 8$), according to the scheme shown in **Figure 3a**. 2-month-old male p16-3MR mice (young; $n = 5$) without treatment and a WT C57BL/6 mouse were used as controls. The vertical color bar indicates luminescence-signal strength. $^{\#}P < 0.05$ versus young mice, $^{\&}P < 0.05$ versus vehicle-treated aged mice; unpaired Student's *t*-test. Scale bars, 15 mm. (**b**–**j**) Aged (21- to 22-month-old) male C57BL/6 mice received vehicle (Veh) or ABT263 (ABT) according to the scheme shown in **Figure 3a** and were analyzed 1 week after the treatment; 2-month-old male C57BL/6 mice without treatment (young) were used as controls. (**b**) Quantification of changes in mRNA levels of *Cdkn2a*, *Tnfa* and *Ccl5* in the lungs of aged (Veh, $n = 11$; ABT, $n = 10$) and young ($n = 9$) mice. (**c**) Scheme for competitive and serial BMT using sorted long-term HSCs (LT-HSCs; $CD34^-CD48^-CD150^+Lin^-Sca1^+c\text{-}Kit^+$). (**d**) Quantification of the percentages of donor-derived total cells, T cells, B cells and M cells in the PB of primary recipients (recipients of donor cells from: young, $n = 11$; vehicle-treated aged, $n = 15$; ABT263-treated aged, $n = 13$; from two independent BMT experiments). Donor cell engraftment in the PB of secondary recipients is shown in **Supplementary Figure 10c**. (**e**) Gating strategy for analysis and isolation of MuSCs by flow cytometry (top) and representative micrographs showing immunostaining for the myogenic transcription factor Pax7 (a biomarker for MuSCs) (bottom). IF, immunofluorescence; MCFC, myogenic colony-forming cell. Scale bars, 20 μm. (**f**) Quantification of MuSCs in muscle tissue. (**g**) Quantification of primary (left) and secondary (right) MCFCs in sorted MuSCs. (**h**,**i**) Quantification of $p16^+$ cells (**h**) and phosphorylated $p38^+$ ($p\text{-}p38^+$) (**i**) cells in MuSCs. (**j**) Quantification of the average number of γ-H2AX foci in MuSCs. $n = 5$, 6, and 6 mice per group for Young, Aged + Veh, and Aged + ABT, respectively, for **f**,**h**,**i**,**j**; 8, 12, and 13 mice per group for **g**. Throughout, data are means ± s.e.m. In **d**, $^{\#}P < 0.05$ versus recipients of donor cells from young mice, $^{\&}P < 0.05$ versus recipients of donor cells from vehicle-treated aged mice; in **g**–**j**, $^{\#}P < 0.05$ versus young mice, $^{\&}P < 0.05$ versus vehicle-treated aged mice; unpaired Student's *t*-test.

of *Cdkn2a*, *Tnfa* (which encodes tumor necrosis factor (TNF)-α) and *Ccl5* (which encodes the chemokine CCL5) in lungs (**Fig. 4b**). In mice, aging is associated with a qualitative, but not a quantitative, reduction in tissue stem cells, including HSCs and MuSCs, which has been attributed in part to stem cell senescence[25,34]. Although it is still a matter of intense debate whether HSCs senesce with age depending on p16 upregulation, HSCs from aged mice consistently exhibit defects in single-cell clonogenicity, long-term repopulating ability and balanced multilineage differentiation[24,25]. All these age-related HSC alterations were attenuated by ABT263 treatment, because HSCs from ATB263-treated aged mice showed a substantial improvement in clonogenic activity in culture, as compared to vehicle-treated aged mice, and were capable of long-term and multilineage engraftment after bone marrow transplantation (**Fig. 4c**,**d** and **Supplementary Fig. 10**). In addition, we studied the effects of ABT263 treatment on MuSCs isolated from the hind limb skeletal muscle of normally aged mice. ABT263 treatment of normally aged mice improved the clonogenicity of isolated MuSCs in culture, as compared to MuSCs isolated from vehicle-treated aged mice (**Fig. 4e**–**g**). This improvement was associated with significant reductions in the number of MuSCs that stained positive for p16, phosphorylated p38 ($p\text{-}p38^+$, a biomarker of senescent MuSCs) and the DNA damage marker γ-H2AX (**Fig. 4e**–**j** and **Supplementary Fig. 11**), which are considered to be senescent MuSCs[34]. These findings suggest that ABT263 treatment of normally aged mice clears senescent HSCs in the bone marrow and MuSCs in the skeletal muscle and rejuvenates the function of the remaining HSCs and MuSCs.

Collectively, our results show that ABT263 is a potent and broad-spectrum senolytic drug, with potential activity as a mitigator of radiation injury, particularly with respect to the late effects of IR that are associated with increases in SC abundance, such as IR-induced long-term bone marrow injury. However, ABT263 has some toxic side effects[35]; in particular, transient thrombocytopenia and neutropenia are the common toxicities associated with ABT263 treatment in patients. Adverse drug effects are hurdles for anti-aging therapies that require long treatment intervals[5,36]. Therefore, it remains to be determined whether ABT263 treatment can be used to delay aging or age-related diseases in normally aged experimental animals or in humans.

METHODS

Methods and any associated references are available in the online version of the paper.

Note: Any Supplementary Information and Source Data files are available in the online version of the paper.

ACKNOWLEDGMENTS

We thank G. van Zant (University of Kentucky) for FBMD-1 stromal cells. This study was supported by the US National Institutes of Health (NIH) grants R01 CA122023 (D.Z.), R01 AI080421 (D.Z.), P20 GM109005 (M.H.-J. and D.Z.) and R37 AG009909 (J. Campisi); a grant from the Edward P. Evans Foundation (D.Z. and M.H.-J.); National Natural Science Foundation of China grant no. 81129020 (D.Z.); China National Program on Key Basic Research Project 2011CB964800-G (A.M.); and an Arkansas Research Alliance Scholarship from the Arkansas Science & Technology Authority (D.Z.).

AUTHOR CONTRIBUTIONS

J. Chang and Y.W. designed, performed and analyzed most of the experiments; L.S., R.-M.L. and M.D. designed, performed and analyzed some experiments; W.F., Y.L., X.W., N.A.-B., K.K. and K.J. performed experiments; N.E.S. interpreted data and revised the manuscript; J. Campisi provided mice, designed the study, analyzed and interpreted data, and revised the manuscript; U.P. and M.H.-J. interpreted data and revised the manuscript; S.D. and A.M. designed the study, analyzed and interpreted data, and revised the manuscript; D.Z. conceived, designed and supervised the study, analyzed and interpreted data, and wrote the manuscript. All authors discussed the results and commented on the manuscript.

COMPETING FINANCIAL INTERESTS

The authors declare competing financial interests: details are available in the online version of the paper.

1. Le, O.N. *et al.* Ionizing radiation–induced long-term expression of senescence markers in mice is independent of p53 and immune status. *Aging Cell* **9**, 398–409 (2010).
2. Muñoz-Espín, D. & Serrano, M. Cellular senescence: from physiology to pathology. *Nat. Rev. Mol. Cell Biol.* **15**, 482–496 (2014).
3. Richardson, R.B. Ionizing radiation and aging: rejuvenating an old idea. *Aging (Albany, NY)* **1**, 887–902 (2009).
4. Shao, L. *et al.* Total body irradiation causes long-term mouse BM injury via induction of HSC premature senescence in an *Ink4a*- and *Arf*-independent manner. *Blood* **123**, 3105–3115 (2014).
5. Tchkonia, T., Zhu, Y., van Deursen, J., Campisi, J. & Kirkland, J.L. Cellular senescence and the senescent secretory phenotype: therapeutic opportunities. *J. Clin. Invest.* **123**, 966–972 (2013).
6. van Deursen, J.M. The role of senescent cells in aging. *Nature* **509**, 439–446 (2014).
7. Baker, D.J. *et al.* Clearance of $p16^{Ink4a}$-positive senescent cells delays aging-associated disorders. *Nature* **479**, 232–236 (2011).
8. Zhu, Y. *et al.* The Achilles' heel of senescent cells: from transcriptome to senolytic drugs. *Aging Cell* **14**, 644–658 (2015).
9. Hayflick, L. & Moorhead, P.S. The serial cultivation of human diploid cell strains. *Exp. Cell Res.* **25**, 585–621 (1961).
10. Serrano, M., Lin, A.W., McCurrach, M.E., Beach, D. & Lowe, S.W. Oncogenic ras provokes premature cell senescence associated with accumulation of p53 and $p16^{INK4a}$. *Cell* **88**, 593–602 (1997).
11. Demaria, M. *et al.* An essential role for senescent cells in optimal wound healing through secretion of PDGF-AA. *Dev. Cell* **31**, 722–733 (2014).
12. Burd, C.E. *et al.* Monitoring tumorigenesis and senescence *in vivo* with a $p16^{INK4a}$-luciferase model. *Cell* **152**, 340–351 (2013).
13. Sorrentino, J.A. *et al.* $p16^{INK4a}$ reporter mice reveal age-promoting effects of environmental toxicants. *J. Clin. Invest.* **124**, 169–173 (2014).
14. Janzen, V. *et al.* Stem cell aging modified by the cyclin-dependent kinase inhibitor $p16^{INK4a}$. *Nature* **443**, 421–426 (2006).
15. Coppé, J.P., Desprez, P.Y., Krtolica, A. & Campisi, J. The senescence-associated secretory phenotype: the dark side of tumor suppression. *Annu. Rev. Pathol.* **5**, 99–118 (2010).
16. Tse, C. *et al.* ABT-263: a potent and orally bioavailable Bcl-2 family inhibitor. *Cancer Res.* **68**, 3421–3428 (2008).
17. Caserta, T.M., Smith, A.N., Gultice, A.D., Reedy, M.A. & Brown, T.L. Q-VD-OPh, a broad spectrum caspase inhibitor with potent antiapoptotic properties. *Apoptosis* **8**, 345–352 (2003).
18. Cory, S. & Adams, J.M. The Bcl2 family: regulators of the cellular life-or-death switch. *Nat. Rev. Cancer* **2**, 647–656 (2002).
19. Czabotar, P.E., Lessene, G., Strasser, A. & Adams, J.M. Control of apoptosis by the BCL-2 protein family: implications for physiology and therapy. *Nat. Rev. Mol. Cell Biol.* **15**, 49–63 (2014).
20. Childs, B.G., Baker, D.J., Kirkland, J.L., Campisi, J. & van Deursen, J.M. Senescence and apoptosis: dueling or complementary cell fates? *EMBO Rep.* **15**, 1139–1153 (2014).
21. Souers, A.J. *et al.* ABT-199, a potent and selective BCL-2 inhibitor, achieves antitumor activity while sparing platelets. *Nat. Med.* **19**, 202–208 (2013).
22. Lessene, G. *et al.* Structure-guided design of a selective Bcl-XL inhibitor. *Nat. Chem. Biol.* **9**, 390–397 (2013).
23. Beerman, I., Maloney, W.J., Weissmann, I.L. & Rossi, D.J. Stem cells and the aging hematopoietic system. *Curr. Opin. Immunol.* **22**, 500–506 (2010).
24. Dykstra, B., Olthof, S., Schreuder, J., Ritsema, M. & de Haan, G. Clonal analysis reveals multiple functional defects of aged murine hematopoietic stem cells. *J. Exp. Med.* **208**, 2691–2703 (2011).
25. Geiger, H., de Haan, G. & Florian, M.C. The aging hematopoietic stem cell compartment. *Nat. Rev. Immunol.* **13**, 376–389 (2013).
26. Shao, L., Luo, Y. & Zhou, D. Hematopoietic stem cell injury induced by ionizing radiation. *Antioxid. Redox Signal.* **20**, 1447–1462 (2014).
27. Fleenor, C.J., Marusyk, A. & DeGregori, J. Ionizing radiation and hematopoietic malignancies: altering the adaptive landscape. *Cell Cycle* **9**, 3005–3011 (2010).
28. Geiger, H., Rennebeck, G. & Van Zant, G. Regulation of hematopoietic stem cell aging *in vivo* by a distinct genetic element. *Proc. Natl. Acad. Sci. USA* **102**, 5102–5107 (2005).
29. Harfouche, G. & Martin, M.T. Response of normal stem cells to ionizing radiation: a balance between homeostasis and genomic stability. *Mutat. Res.* **704**, 167–174 (2010).
30. Testa, N.G., Hendry, J.H. & Molineux, G. Long-term bone marrow damage in experimental systems and in patients after radiation or chemotherapy. *Anticancer Res.* **5**, 101–110 (1985).
31. Gale, R.P. in *Hematopoiesis: Long-term Effects of Chemotherapy and Radiation* (eds. Testa, N.G. & Gale, R.P.) 63–73 (Marcel Dekker, Inc., New York, 1988).
32. Lohrmann, H.P.E. & Schreml, W. in *Hematopoiesis: Long-term Effects of Chemotherapy and Radiation* (eds. Testa, N.G. & Gale, R.P.) 325–337 (Marcel Dekker, Inc., New York, 1988).
33. Carbonneau, C.L. *et al.* Ionizing radiation-induced expression of *Ink4a*/*Arf* in murine bone marrow–derived stromal cell populations interferes with bone marrow homeostasis. *Blood* **119**, 717–726 (2012).
34. Blau, H.M., Cosgrove, B.D. & Ho, A.T. The central role of muscle stem cells in regenerative failure with aging. *Nat. Med.* **21**, 854–862 (2015).
35. Rudin, C.M. *et al.* Phase 2 study of single-agent navitoclax (ABT-263) and biomarker correlates in patients with relapsed small cell lung cancer. *Clin. Cancer Res.* **18**, 3163–3169 (2012).
36. Le Couteur, D.G., McLachlan, A.J., Quinn, R.J., Simpson, S.J. & de Cabo, R. Aging biology and novel targets for drug discovery. *J. Gerontol. A Biol. Sci. Med. Sci.* **67**, 168–174 (2012).

ONLINE METHODS

Cells. Human WI-38 (WI-38, catalog no. CCL-75) and IMR-90 fibroblasts (IMR-90, catalog no. CCL-186) and human renal epithelial cells (RECs, catalog no. PCS-400-012) were originally obtained from the American Type Culture Collection (Manassas, VA, USA). Mouse embryonic fibroblasts (MEFs) were isolated from mouse embryos as previously described[37]. All cells were cultured in a complete cell culture medium (CM) (Dulbecco's Modified Eagle Medium supplemented with 10% FBS, 100 U/ml penicillin and 100 μg/ml streptomycin (all from Atlanta Biologicals, Norcross, GA, USA)) in a humidified incubator at 37 °C and 5% CO_2. To avoid cells that were undergoing replicative senescence, low-passage WI-38 (<25 passages), IMR-90 (<25 passages), RECs (<25 passages), and MEFs (<3 passages) cells were used as normal controls or for the induction of senescence. To induce replicative senescence, WI-38 cells were routinely subcultured until they stopped dividing and became senescent, after approximately 38 passages or 60 population doublings (**Supplementary Fig. 1a**)[38]. To induce cellular senescence by ionizing radiation (IR), cells at about 70% confluence were exposed to 10 Gy of IR in a J.L. Shepherd Model Mark I ^{137}Cesium γ-irradiator (J.L. Shepherd, Glendale, CA, USA) at a dose rate of 1.080 Gy/min. Three days after irradiation, cells were passaged once at a 1:3 dilution, and they became fully senescent 7 d after irradiation, as shown in **Supplementary Figure 1a** (ref. 38). To induce cellular senescence by ectopic expression of *Ras*, WI-38 cells were infected with retroviruses containing pBabe-H-*Ras* or the pBabe-puro control vector (Addgene, Cambridge, MA, USA)[10,38]. Two days after viral infection, transfected cells were selected by incubation with puromycin (2 μg/ml) (Invitrogen, Grand Island, NY, USA) for 5 d; *Ras*-transfected cells but not control vector–transfected cells then became senescent (**Supplementary Fig. 1a**). Until they were used for experiments, SCs were maintained in culture for a few days (but <7 d) by changing the culture medium every 3 d.

Cell viability assays. Cells were seeded into wells of a 24- or 48-well plate. After overnight incubation, they were treated with vehicle (0.1% DMSO or PBS) or compounds (listed in **Supplementary Tables 1** and **2**) at increasing concentrations and for various periods of times. The cells were digested with 0.25% trypsin and 1 mM EDTA, and harvested in PBS containing 2% FBS. After incubation with propidium iodide (PI, 100 ng/ml) in PBS at room temperature for 1 min, cells were centrifuged at 1,200 r.p.m. for 6 min to remove PI and then resuspended in PBS containing 2% FBS for analysis using a BD LSR II flow cytometer (BD Biosciences, San Jose, CA, USA). Viable cells (PI^- cells) were analyzed by flow cytometry at a constant flow rate and calculated as a percentage of control cells treated with vehicle using the formula: percentage of control = $(N_{drug}/N_c) \times 100$, where N_{drug} and N_c represent the absolute number of PI^- viable cells for drug-treated and vehicle-treated cells, respectively.

Calculation of EC_{50} values. Dose-response curves were generated for each tested compound and the half-maximal inhibitory concentrations (EC_{50} values) were calculated by Probit analysis[39].

SA–β-galactosidase staining, BrdU incorporation assays and apoptosis assays. SA–β-gal staining was done using a SA–β-gal staining kit (catalog no. 9860; Cell Signaling Technology, Danvers, MA, USA) according to the manufacturer's instructions. SCs were identified as blue-stained cells under light microscopy. A total of 1,000 cells were counted in 20 random fields on a slide to determine the percentage of SA–β-gal^+ cells[38]. Flow SA–β-gal staining assay was performed by flow cytometry using an ImaGene Green C_{12}FDG lacZ gene expression kit from Molecular Probes (Life Technologies, Carlsbad, CA), according to the manufacturer's instructions and the protocols reported previously[40].

A BrdU incorporation assay was used to determine cellular senescence as previously described[41]. Apoptosis was determined by flow cytometry as previously described[4].

Microscopy. Cells were viewed and photographed using an Axioplan research microscope (Carl Zeiss Inc., Jena, Germany) equipped with a 100-W mercury light source. Images were captured with a Dage CCD100 integrating camera (Dage-MTI, Michigan, USA) and a Flashpoint 128 capture board (Integral Technologies, Indianapolis, Indiana, USA). The captured images were processed using Image Pro Plus software (Media Cybernetics, Rockville, Maryland, USA) and displayed with Adobe Photoshop V6.0.

Western blot analysis. Cells (1×10^6) were lysed in 100 μl lysis buffer (20 mM Tris-HCl pH 7.4, 150 mM NaCl, 1 mM EDTA, 1 mM EGTA, 10% glycerol, 1% NP-40, 0.1 M NaF, 1 mM DTT, 1 mM PMSF, 1 mM sodium vanadate and 2 μg/ml leupeptin and aprotinin). An equal amount of protein (25–50 μg/lane) from each cell extract was resolved on a 12% SDS-PAGE gel. Proteins were blotted to a NOVEX NC membrane (Life Technologies) by electrophoresis. A mixture of the cell lysates from etoposide-treated Jurkat cells (prepared by the authors) and cytochrome c–treated Jurkat cells (obtained from Cell Signaling, Danvers, MA, USA) was used as a positive control for the blots presented in **Figure 2d**,**e**. The membranes were blocked with TBS-T blocking buffer (5% nonfat milk in 25 mM Tris-HCl pH 7.4, 3 mM KCl, 140 mM NaCl and 0.05% Tween) and subsequently probed with primary antibodies at a predetermined optimal concentration overnight at 4 °C or for 1 h at room temperature. After extensive washing with TBS-T, the membranes were then incubated with an appropriate peroxidase-conjugated secondary antibody (Jackson Immuno Research Europe, Suffolk, UK) for 1 h at room temperature. After three washes with TBS-T, the proteins of interest were detected using the ECL Western Blotting Detection Reagents (catalog no. WBKLS0100, EMD Millipore, Newmarket, Suffolk, UK) and recorded by exposure of the blots to X-ray film (Pierce Biotech, Rockford, IL, USA). Information on all antibodies used in western blot analyses is listed in **Supplementary Table 3**.

Knockdown of *BCL2* and/or *BCL2L1* with short hairpin RNAs (shRNAs). Control lentiviral pLKO.1 vectors and pLKO.1 vectors containing shRNAs specific for human *BCL2* (RHS4533–EG596) and *BCL2L1* (RHS4533–EG598) were obtained from Thermo Fisher Scientific, Inc. (Waltham, MA, USA). Viral particles were produced as described above. To establish stable *BCL2*- and/or *BCL2L1*-knockdown WI-38 cell lines, WI-38 cells were infected twice with the viral particles under centrifugation (900*g*) at 32 °C for 30 min. Stably transduced cells were selected with puromycin (2 mg/ml). *BCL2* and/or *BCL2L1* knockdown was confirmed by western blot before the cells were used in an experiment.

Mice. Young (approximately 2-month-old) male C57BL/6J (CD45.2) mice and B6.SJL–*Ptprc*^{a}*Pepc*^{b}/BoyJ (CD45.1) (a C57BL/6 congenic strain of mice used as recipients for BMT; *Ptprc*, protein tyrosine phosphatase receptor type C; *Pepc*, peptidase C) mice were purchased from Jackson Laboratory (Bar Harbor, MA, USA). p16-3MR transgenic mice were bred at the University of Arkansas for Medical Sciences' (UAMS) Association for the Assessment and Accreditation of Laboratory Animal Care International (AAALAC)-certified animal facility as described previously[11]. Mice were randomly assigned to 4 or 5 mice per cage, were housed at the UAMS AAALAC-certified animal facility and received food and water *ad libitum*. Aged male C57BL/6J mice (approximately 20 months old) were obtained from the aged-rodent colonies of the National Institute on Aging (https://www.nia.nih.gov/research/scientific-resources#rodent). The mice were housed in the University of North Carolina at Chapel Hill's (UNC) barrier facility on a standard diet along with a group of young male C57BL/6 mice as controls. The mice used for all of the experiments were randomly assigned to a treatment group. For animal studies, sample sizes were estimated according to our previous experience. Mice with tumors and/or leukemia were excluded from experiments and analyses. All animal work was approved and done in accordance with the UAMS and UNC Institutional Animal Care and Use Committees.

Total body irradiation (TBI) and treatment with ABT263 and ganciclovir (GCV). Male C57BL/6J and p16-3MR transgenic mice at 2–3 months of age were exposed to sham irradiation as controls or a sublethal dose (6 Gy) of TBI in a J.L. Shepherd Model Mark I ^{137}Cesium γ-irradiator (J.L. Shepherd) at a dose rate of 1.080 Gy/min. 8 or 16 weeks after TBI, mice were treated with vehicle (either PBS or ethanol:polyethylene glycol 400:Phosal 50 PG (a standardized phosphatidylcholine (PC) concentrate with at least 50% PC

doi:10.1038/nm.4010

and propylene glycol, Phospholipid Gmbh, Cologne, Germany) at 10:30:60), ABT263 (in ethanol:polyethylene glycol 400:Phosal 50 PG), or GCV (in PBS). ABT263 was administered to mice by gavage at 50 mg per kg body weight per day (mg/kg/d) for 7 d per cycle for two cycles with a 2-week interval between the cycles. GCV was administered to mice by intraperitoneal (i.p.) injection at 25 mg/kg/d for 5 d per cycle for two cycles with a 2-week interval between the cycles. Luminescence imaging was performed on p16-3MR mice 1 d after the last treatment with vehicle, ABT263 or GCV, as described below. The day after imaging, mice were killed by CO_2 suffocation followed by cervical dislocation. Various tissues were harvested for immediate tissue luminescence imaging, as described below, or for RNA extraction to analyze SASP. Groups of young C57BL/6 and p16-3MR transgenic mice were also killed 5 weeks after vehicle, ABT263 or GCV treatment to harvest bone marrow cells (BMCs) for the various assays described below. In addition, groups of young (2- to 3-month-old) and aged (21- to 22-month-old) male C57BL/6 and p16-3MR transgenic mice were treated with vehicle or ABT263 and analyzed as described above.

Bioluminescence assay. For measurement of *in vivo* luminescence, mice were injected i.p. with 250 µl of Xenolight RediJect Coelenterazine h (100 µg/ml, PerkinElmer, Waltham, MA, USA). Five minutes after the injection, mice were anesthetized with 4% isoflurane gas at 1 liter/min oxygen flow. Luminescence images were acquired using a Xenogen IVIS-200 Optical *in vivo* Imaging System equipped with Living Image Version 4.3.1 software (Caliper Life Sciences, Hopkinton, MA, USA). All image scans were acquired with an E field of view at 15–20 min after the injection; the mice were kept under 1.5% isoflurane gas at 1 liter/min oxygen flow.

For tissue luminescence imaging, tissues harvested from euthanized mice were immediately soaked in prewarmed (37 °C) PBS with 2% FBS and a 1:10 dilution of Xenolight RediJect Coelenterazine h for 10 min. Tissues were then transferred into a new 35-mm dish, and luminescence images were acquired using a Xenogen IVIS-200 Optical *in vivo* Imaging System at 12–15 min after the tissue had been soaked in substrate solution.

Isolation of bone marrow mononuclear cells (BM-MNCs), lineage-negative hematopoietic cells (Lin$^-$ cells), HSCs and LT-HSCs. BMCs were harvested, bone marrow mononuclear cells (BM-MNCs) and lineage-negative hematopoietic (Lin$^-$) cells were isolated, and HSCs (CD150$^+$CD48$^-$Lin$^-$Sca1$^+$c-Kit$^+$, also referred to as CD150$^+$CD48$^-$LSK, cells) and LT-HSCs (CD34$^-$CD48$^-$CD155$^+$ LSK cells) were sorted by an Aria II cell sorter (BD Biosciences) as described previously[4]. Information for all of the antibodies used in cell isolation and sorting is listed in **Supplementary Table 4**.

B cell analysis. BM-MNCs (1×10^6) were incubated with FITC-labeled anti-CD93, APC-labeled anti-IgM and PE-labeled anti-B220 at 4 °C for 30 min and then washed with PBS containing 0.25 µg/ml PI. Various B cell populations were analyzed using a BD LSRII flow cytometer (BD Biosciences).

Colony-forming cell assay in single-HSC liquid culture. The assay was done as described previously[4]. Briefly, single HSCs were directly sorted into wells of round-bottom 96-well plates. They were cultured in RPMI 1640 culture medium supplemented with 10% FCS, 50 ng/ml of mSCF, mFlt-3, mTPO and mGM-CSF, 20 ng/ml of mouse interleukin (IL) 3, and 5 U/ml mEPO (**Supplementary Table 2**) in the absence or presence of 1.25 µM ABT263. Freshly prepared medium was added every 3 d. After 14 d of culture, the numbers of cells produced by each HSC were counted. Cells that produced more than 10,000 cells were scored as colony-forming cells.

Cobblestone area–forming cell (CAFC) assay. The CAFC assay for BMCs was done as described previously[4,42]. For the single-HSC CAFC assay, single LT-HSCs from young and aged C57BL/6 mice treated with vehicle or ABT263 were directly sorted into wells of round-bottom 96-well plates containing FBMD-1 stromal cells. CAFCs were scored by bright-field microscopy after 5–8 weeks of incubation as described previously[24].

Competitive repopulation assay (CRA) and serial bone marrow transplantation (BMT). CD45.2 mice were exposed to a sublethal dose (6.0 Gy) of TBI or sham irradiation and then treated with vehicle or ABT263 as shown in **Figure 3a**,**g**. BMCs were isolated and mixed with 2×10^5 competitive BMCs pooled from three CD45.1 mice. The cell mixture was then transplanted into lethally irradiated (9.5 Gy TBI) CD45.1 recipients via retro-orbital injection of the venous sinus. For the normal aging study, 50 freshly sorted LT-HSCs from young and aged C57BL/6 mice treated with vehicle or ABT263 were mixed with 3×10^5 competitive BMCs pooled from three CD45.1 mice, and the cell mixture was then transplanted into lethally irradiated CD45.1 recipients via retro-orbital injection of the venous sinus. Donor-cell engraftment in the recipients was analyzed at various times after transplantation as previously described[4,42]. For secondary BMT, 1×10^6 BMCs were harvested from each primary recipient 4 months after primary BMT and were then transplanted into a lethally irradiated recipient as described above. Donor-cell engraftment in both primary and secondary recipient peripheral blood was analyzed as previously described[4,42].

Cell cycle and DNA damage analysis. Lin$^-$ cells were stained with antibodies against various HSC cell-surface markers and then fixed and permeabilized using Fixation-Permeabilization Solution (BD-Pharmingen, San Diego, CA). Subsequently, the cells were stained with anti-Ki67-FITC, anti–phospho–histone H2AX (γ-H2AX) (Ser139)–Alexa Fluor 647, and 7-aminoactinomycin D (7-AAD) and then analyzed by flow cytometry as previously described[4].

Isolation of bone stromal cells. Femur, tibia and pelvic bones were harvested from euthanized mice and cleaned by removing surrounding tissue and by flushing out bone marrow cells. The bones were cut into small (<1-mm long) pieces using scissors and then digested with 0.1% collagenase I and 15 µg/ml DNAse I (Sigma, St. Louis, MO, USA) in PBS with 15% FBS at 37 °C for 1 h. Cells were collected after removing bone debris and filtering through a 40-µm filter. CD45$^-$Lin$^-$PI$^-$ bone stromal cells were harvested by cell sorting after staining with APC-conjugated anti-CD45, biotin-conjugated anti-CD11b, CD3ε, Gr-1, B220 and Ter119, FITC-conjugated streptavidin and PI.

Isolation of muscle stem cells (MuSCs). Skeletal muscles, harvested from the hind legs of mice after euthanization, were torn into small pieces with forceps and were then digested with 0.2% type II collagenase in F10 medium containing 10% horse serum (Thermo Fisher Scientific) for 90 min at 37 °C. After washing three times with PBS, single myofibers were digested further with 0.1% type II collagenase and 0.05% dispase (Thermo Fisher Scientific) in PBS for 30 min at 37 °C to separate myofiber-associated cells (containing MuSCs) from myofibers. Myofiber-associated cells were filtered through a 70-µm cell strainer (Thermo Fisher Scientific), harvested by centrifugation (500*g*, 8 min), and stained with antibodies to CD45, Mac1, Sca1, CXCR4 and β1-integrin for cell sorting and analysis as described previously[43,44]. Information for all of the antibodies used for staining is provided in **Supplementary Table 4**.

Myogenic colony-forming cell assay for MuSCs. Single MuSCs were deposited into wells of collagen- and laminin-precoated 96-well plates (Corning Inc., NY, USA) at 1 cell per well by an Aria II cell sorter (BD Biosciences), as described previously[43,44]. The cells were cultured in F10 medium supplemented with 20% horse serum and 5 µg/ml basic fibroblast growth factor (bFGF; Thermo Fisher Scientific) and were fed every day with freshly prepared bFGF. Wells containing myogenic colonies were scored by bright-field microscopy after 6 d of culture to determine the number of primary myogenic colony-forming cells (MCFCs)[43,44]. Cells were harvested from individual wells containing myogenic colonies, diluted 1:5 with F10 medium supplemented with 20% horse serum and 5 µg/ml bFGF, and then reseeded into five wells of collagen- and laminin-precoated 96-well plates for quantification of secondary MCFCs in a manner similar to that for primary MCFCs.

Analysis of senescent MuSCs by p38 phosphoflow assay. Myofiber-associated cells were stained with antibodies against various MuSC surface markers, fixed and permeabilized using Fixation-Permeabilization Solution (BD-Pharmingen), as shown in **Figure 4e**. Subsequently, the cells were stained with anti-p-p38 (#4551; Cell Signaling, Danvers, MA, USA) and analyzed by flow cytometry.

Analysis of Pax7, p16 and γ-H2AX expression in MuSCs by immunostaining. Approximately 2,000 freshly sorted MuSCs were spun on a slide for immunostaining by cytospin. After fixation with 4% paraformaldehyde (PFA) for 15 min at room temperature, cells were incubated in 0.1% Triton X-100 at room temperature for half an hour. After washing with PBS and a 60-min incubation in PBS with 1% bovine serum albumin, cells were incubated overnight at 4 °C with antibodies to p16, γ-H2AX or Pax7 (**Supplementary Table 4**), and then incubated with the corresponding secondary antibodies, with extensive washing between each step. The nuclear DNA of the cells was counterstained with DAPI (Sigma, St. Louis, MO, USA). The cells were viewed and photographed using an Axioplan research microscope as described above. A total of more than 100 cells per slide were counted in >30 random fields on a slide to determine the percentage of $p16^+$ cells and the number of γ-H2AX foci for calculation of the average number of γ-H2AX foci/cell.

Quantitative PCR (qPCR). Total cellular RNA was extracted and reverse transcription was performed as described previously[4]. To measure *CDKN2A* and *Cdkn2a* mRNA expression in WI-38 cells and mouse tissue, respectively, qPCRs were run with TaqMan qPCR reagents and primers (**Supplementary Table 5**) from Applied Biosystems. Human *GAPDH* and mouse *Hprt* were used as internal controls. Briefly, 1 µl cDNA was mixed with 10 µl TaqMan Universal Mastermix (Invitrogen) and 1 µl of TaqMan primers. Samples were added to 8 µl of water (for a total volume of 20 µl) and used for qPCR (50 °C for 2 min, 95 °C for 10 min, 40 × (95 °C for 15 s and 60 °C for 1 min)). All reactions were run in triplicate on an ABI StepOnePlus Real-Time PCR System (Applied Biosystems).

To measure *CDKN1A* and *GAPDH* mRNA expression in WI-38 cells and *Cdkn1a* and SASP gene expression (including *Il1a*, *Il1b*, *Il6*, *Tgfb1*, *Tnfa*, *Ccl5* and *Cxcl10* mRNA) in mouse tissues, bone marrow HSCs and bone stromal cells, the SYBR assay kit was used (Applied Biosystems). Briefly, 1 µl cDNA was mixed with 7.5 µl SYBR Green PCR Master Mix and 0.2 µl of primers (**Supplementary Table 5**). Samples were then added to 6.30 µl of water (for a total volume of 15 µl). qPCR conditions were as follows: 95 °C for 10 min, 40 × (95 °C for 15 s and 60 °C for 1 min), 95 °C for 15 min, 60 °C for 60 min, 95 °C for 15 min. All reactions were run in triplicate on an ABI StepOnePlus Real-Time PCR System.

Statistical analysis. The data displayed normal variance. No statistical method was used to predetermine sample size. The experiments were not randomized, except for the *in vivo* animal studies with mice as described above. The investigators were not blinded to allocation during experiments and outcome assessment. The data were analyzed by analysis of variance (ANOVA) using GraphPad Prism from GraphPad Software (San Diego, CA). In the event that ANOVA justified post hoc comparisons between group means, these were conducted using Neuman-Keuls or Tukey's multiple-comparisons test. $P < 0.05$ was considered to be significant.

37. Jozefczuk, J., Drews, K. & Adjaye, J. Preparation of mouse embryonic fibroblast cells suitable for culturing human embryonic and induced pluripotent stem cells. *J. Vis. Exp.* **64**, 3854 (2012).
38. Wang, Y., Scheiber, M.N., Neumann, C., Calin, G.A. & Zhou, D. MicroRNA regulation of ionizing radiation–induced premature senescence. *Int. J. Radiat. Oncol. Biol. Phys.* **81**, 839–848 (2011).
39. Finney, D.J. *Probit Analysis* (Cambridge University Press, Cambridge, UK, 1952).
40. Debacq-Chainiaux, F., Erusalimsky, J.D., Campisi, J. & Toussaint, O. Protocols to detect senescence-associated β-galactosidase (SA–β-gal) activity, a biomarker of senescent cells in culture and *in vivo*. *Nat. Protoc.* **4**, 1798–1806 (2009).
41. Wang, Y., Meng, A. & Zhou, D. Inhibition of phosphatidylinostol 3-kinase uncouples H_2O_2-induced senescent phenotype and cell cycle arrest in normal human diploid fibroblasts. *Exp. Cell Res.* **298**, 188–196 (2004).
42. Wang, Y., Schulte, B.A., LaRue, A.C., Ogawa, M. & Zhou, D. Total body irradiation selectively induces murine hematopoietic stem cell senescence. *Blood* **107**, 358–366 (2006).
43. Cerletti, M., Jang, Y.C., Finley, L.W., Haigis, M.C. & Wagers, A.J. Short-term calorie restriction enhances skeletal muscle stem cell function. *Cell Stem Cell* **10**, 515–519 (2012).
44. Cosgrove, B.D. *et al.* Rejuvenation of the muscle stem cell population restores strength to injured aged muscles. *Nat. Med.* **20**, 255–264 (2014).

doi:10.1038/nm.4010